Second Harmonic Generation of Femtosecond Pulses at the Boundary of a Nonlinear Dielectric

M. Mlejnek, E. M. Wright, and J. V. Moloney
Arizona Center for Mathematical Sciences and Optical Sciences Center, University of Arizona, Tucson, Arizona 85721

N. Bloembergen
Division of Applied Sciences, Harvard University, Pierce Hall, Cambridge, Massachusetts 02138
(Received 10 February 1999)

Using full vector Maxwell simulations we elucidate a fundamental source of temporal splitting of the second harmonic field generated by a femtosecond fundamental pulse under phase-mismatched conditions. One component of the generated field propagates at the second harmonic group velocity while the other is driven by the fundamental field and propagates at the fundamental group velocity. We analyze the conditions under which the temporal splitting should be observable.

PACS numbers: 42.65.Ky, 03.50.De

Although almost 40 years have passed since Franken and co-workers [1,2] first demonstrated second harmonic generation (SHG) and rectification of light, the topic of SHG, in particular, of short pulses, continues to receive much attention, especially in phase-matched and quasi-phase-matched conditions [3–6], because of significant applications. Most papers use the slowly varying envelope approximation to discuss the growth of the second harmonic amplitude, starting from zero at the boundary of the nonlinear crystal ($z = 0$). This approach would be strictly valid if the dielectric constant would slowly increase over many optical wavelengths eliminating reflection. It is well known that rigorous solutions of Maxwell's equations at a sharp boundary with a discontinuity in the linear and nonlinear susceptibilities require the presence of both reflected and transmitted fields.

Rigorous solutions for second harmonic fields valid in steady-state conditions (very long pulses) were given by Bloembergen and Pershan [7] shortly after the initial experiments. It was shown that the total second harmonic field consists of a reflected wave in the linear medium (usually air or vacuum) and two transmitted waves in the nonlinear medium which respectively represent the solutions of the homogeneous and the inhomogeneous wave equations. The latter is driven by the nonlinear polarization and has a wave vector $2\vec{k}_1$ equal to twice the wave vector of the fundamental wave in the nonlinear medium. The homogeneous solution has a wave vector $|\vec{k}_2| = 2\omega n(2\omega)/c$, where $n(2\omega)$ is the index of refraction at the second harmonic frequency. For normal incidence the interference between the homogeneous and inhomogeneous solution leads to the occurrence of Maker-Terhune fringes in the second harmonic intensity as a function of the distance z traveled in the nonlinear medium [8]. For large angles of incidence the beams corresponding to the homogeneous and inhomogeneous solutions are separated in space for non-phase-matched conditions [9].

Recently exact solutions have been obtained for a femtosecond pulse incident from vacuum onto a nonlinear dielectric with a phase mismatch between fundamental and second harmonic caused by birefringence [10]. Using numerical simulations based on the full vector Maxwell equations, we elucidate in this Letter a fundamental source of temporal splitting of the second harmonic field generated using ultrashort pulses which extends beyond the regime of the usual slowly varying envelope approximation. In the early stages before pulse splitting the two second harmonic components beat together in space to yield the Maker-Terhune fringes, whereas these components separate for long distances. We show that this phenomenon should be observable with current lasers and materials.

For the sake of concreteness consider the experimental situation shown in Fig. 1. For sufficient phase mismatch the second harmonic intensity always remains very small compared to the fundamental intensity, and we hereafter assume the fundamental is undepleted. The fundamental pulse is polarized along the $[1, 1, 0]$ crystallographic axis labeled as the x direction of a KDP crystal, and induces

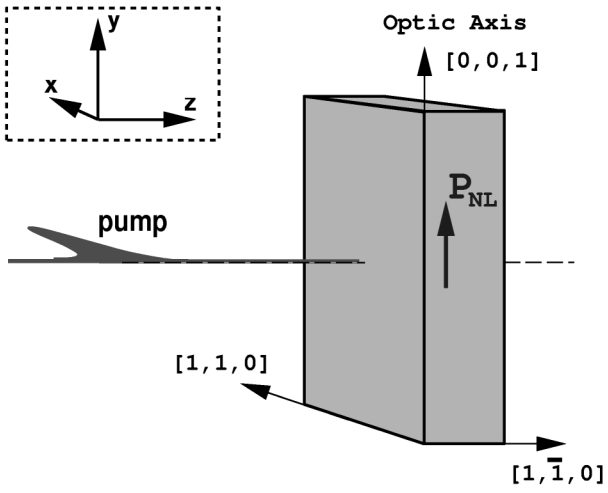

FIG. 1. The incident pulse on the KDP is polarized as an ordinary ray. It creates a nonlinear polarization along the optic axis.

 0031-9007/99/83(15)/2934(4)$15.00

a nonlinear polarization along the $[0, 0, 1]$ or y direction, i.e., parallel to the optic axis,

$$P_y^{NL} = \epsilon_0 \chi^{(2)} E_x^2. \tag{1}$$

The pulses propagate along the crystallographic $[1, \bar{1}, 0]$ or z direction. Assume initially that there is no color dispersion: This is clearly not realistic, but the consequences of dispersion will be discussed later. In this case the induced nonlinear pulse satisfies the wave equation (we assume one spatial dimension z, i.e., plane waves, or alternatively we ignore diffraction, $|\vec{k}_T| \ll k_z$, where $\vec{k}_T$ and k_z are transverse and longitudinal wave vectors, respectively, and treat each transverse dimension separately)

$$\frac{\partial^2 E_y}{\partial z^2} - \frac{1}{v_y^2} \frac{\partial^2 E_y}{\partial t^2} = \mu_0 \frac{\partial^2 P_y^{NL}}{\partial t^2} \tag{2}$$

with

$$P_y^{NL}(z, t) = \epsilon_0 \chi^{(2)} A_x^2 f^2(t - z/v_x) \tag{3}$$

and $v_y = c/n_{||}(2\omega) = c/n_{||}(0)$. Note that all quantities are real. The fundamental pulse in the medium has an amplitude A_x and a shape $f(t - z/v_x)$ with $v_x = c/n_\perp(\omega)$. The nonlinear source term has a shape $f^2(t - z/v_x)$ which propagates at the fundamental velocity v_x. A special solution of the inhomogeneous Eq. (2) is

$$E_y^{\text{inh}}(z, t) = \frac{\chi^{(2)} A_x^2}{n_\perp^2 - \epsilon_{||}} f^2(t - z/v_x). \tag{4}$$

The homogeneous equation, when the right hand side in Eq. (2) is put equal to zero, has a general solution

$$E_y^{\text{hom}}(z, t) = A_y^T g^T(t - z/v_y) \tag{5}$$

with arbitrary amplitude A_y^T. The reflected pulse obeys the wave equation for linear incident medium and has the general solution

$$E_y^{\text{refl}}(z, t) = A_y^R g^R(t + z/v_0), \qquad v_0 = c/n_0, \tag{6}$$

with n_0 the index of refraction of the incident medium. The continuity of the tangential components E_y and H_x at the boundary can be satisfied for $z = 0$ at all times [7] if we take

$$g^T(t) = g^R(t) = f^2(t) \quad \text{for all } t,$$

$$A_y^R = \frac{\chi^{(2)} A_x^2}{(n_{||} + n_\perp)(n_{||} + n_0)}, \tag{7}$$

$$A_y^T = -\frac{\chi^{(2)} A_x^2}{n_\perp^2 - \epsilon_{||}} \frac{n_\perp + n_{||}}{n_0 + n_{||}}. \tag{8}$$

The main consequences of solutions (3)–(8) are that the homogeneous and inhomogeneous second harmonic pulse components travel at different velocities ($v_x \neq v_y$) and must therefore separate at sufficiently large distances, i.e., pulse splitting of the second harmonic field, and the unipolarity of the generated pulses since they are both proportional to $f^2(t), f(t)$ being real. The unipolar nature of the generated fields arises here since we ignored color dispersion, and the second harmonic field and low frequency field arising from optical rectification therefore propagate together.

These expectations are readily verified by numerically solving the Maxwell equations for short plane wave incident pulses and the geometry of Fig. 1 (but without the undepleted pump beam approximation). In particular, for illustrative purposes we chose a birefringent medium with no color dispersion $n_{||} = n_y = 1.5$, $n_\perp = n_x = 2.5$, and an initial Gaussian fundamental pulse polarized along the x direction, $E_x(z, t) = A_x \exp[(t - z/v_0)^2/t_p^2] \cos[\omega(t - z/v_0)]$, localized in the vacuum, with $t_p \simeq 12$ fs, $\omega = 1.77 \times 10^{15}$ s^{-1}, and amplitude such that $\chi^{(2)} A_x \simeq 5 \times 10^{-4}$. The situation after propagation over a distance in the nonlinear medium sufficient to separate the homogeneous (free) and inhomogeneous (traveling at the speed of the fundamental pulse) solution is shown in Fig. 2. Here we observe both the temporal splitting and unipolarity of second harmonic pulses.

We next turn to the issue of color dispersion for short pulse SHG. Most birefringent ionic crystals, which are transparent in the visible, and crystals lacking a center of inversion symmetry generally have significant dispersive and absorptive features due to optically active infrared modes causing the dielectric constant at low frequencies to be significantly larger than the square of the index of refraction at optical frequencies. For KDP and $\omega = 2.356 \times 10^{15}$ s^{-1}, $\epsilon_{||}(0) \simeq 17$ [11], while $n_{||}^2(2\omega) \simeq 2.226$. The value of $\epsilon_{||}(0)$ might not be reliable because it is hard to obtain experimentally (compare the measurements in Refs. [11,12]). We include these infrared resonances using a harmonic oscillator model for the linear optical response of KDP, and the permittivity for the extraordinary wave is shown in Fig. 3. The corresponding linear polarization incorporated into our Maxwell equation solver is then a convolution of the

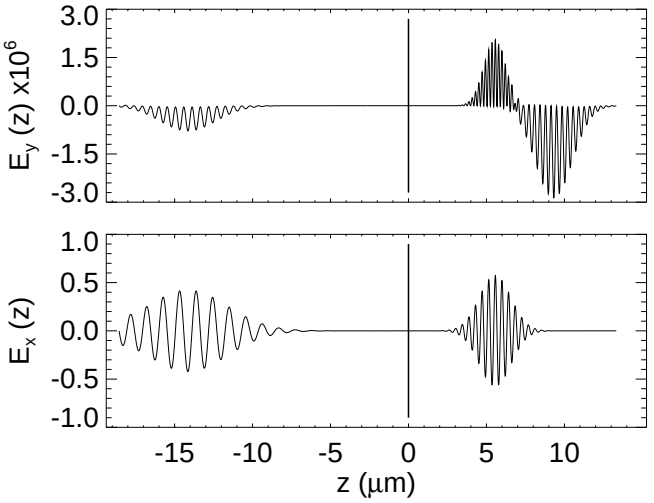

FIG. 2. The fundamental pulses in reflection and transmission (bottom) and the second harmonic and rectified pulses (top), when the inhomogeneous and homogeneous solution in the medium have separated. Vertical line at $z = 0$ μm indicates the boundary between the incident linear medium and the nonlinear dielectric.

electric field with the response function obtained via Fourier transformation of the linear optical susceptibility.

In our numerical simulations we used again as an initial condition a Gaussian pulse incident at the boundary, now with $t_p \simeq 4.3$ fs, carrier frequency $\omega = 2.356 \times 10^{15}\ \mathrm{s}^{-1}$ (corresponding vacuum wavelength $\lambda_0 = 800$ nm), and amplitude such that $\chi^{(2)}A_x \simeq 2.7 \times 10^{-5}$. The second harmonic pulses become completely separated upon propagation as shown in Fig. 4, which incorporates the effects of color dispersion. Thus, we see that the temporal pulse splitting phenomenon illustrated in Fig. 2 in the absence of dispersion can appear even in the presence of color dispersion. In addition, note that in the presence of the material dispersion the low frequency tail accompanying the second harmonic pulses has a wavelength of a few micrometers, longer wavelengths having been absorbed or strongly dispersed.

Before the temporal separation, the pulses interfere and Maker-Terhune-type oscillations can be observed in the computer solution in Fig. 5, which shows a series of time snapshots of the transmitted second harmonic and low frequency fields. These oscillations in amplitude gradually disappear as the pulses separate, and the amplitude of the separated pulses is about a half of the maximum amplitude of the Maker-Terhune fringes. The coherence length is defined by the distance at which the first maximum in the Maker-Terhune fringe pattern occurs, or $l_{\mathrm{coh}} = \lambda_0/4|n_{||} - n_{\perp}|$, which yields for our parameters $l_{\mathrm{coh}} \simeq 8.7\ \mu$m. The separation length at which the homogeneous and inhomogeneous pulse solutions are no longer overlapping is defined by

$$l_{\mathrm{sep}} \simeq \frac{v^2}{|\Delta v|}(2t_p) \simeq \frac{4}{\pi} l_{\mathrm{coh}}(\omega t_p), \tag{9}$$

where $2t_p$ is roughly the pulse duration, v is the pulse velocity, and $\Delta v = v_x - v_y$. Note that the separation length is always larger than the coherence length because typically $\omega t_p \gg 1$. For a pulse duration $2t_p \simeq 8.6$ fs, $l_{\mathrm{sep}} \simeq 110\ \mu$m.

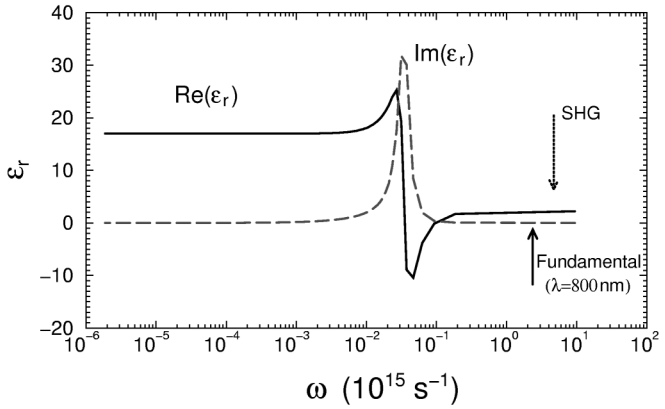

FIG. 3. Low frequency color dispersion in ionic crystals. This dielectric constant models the linear response in the KDP's extraordinary polarization direction.

As a consequence of the infrared resonances the low frequency or rectified components of the homogeneous pulse solution in the material will separate from the second harmonic components, and this will compromise the observability of the unipolar solutions. Furthermore, infrared absorption causes the low frequency components in the homogeneous pulse solutions to diminish. The magnitude of the low frequency components in the driven, or inhomogeneous, solution will also be reduced considerably, when the absorption depth is comparable to or shorter than the coherence length. The imaginary component of the index of refraction is then larger than the difference in the real parts, which occurs in the expression for the inhomogeneous solution given by Eq. (4). The detailed characteristics of infrared dispersion will lead to complex distortions in the propagation of the low frequency components in the pulses which will be completely separated from the second harmonic components. An example of this behavior is shown in Fig. 4, which shows the free and driven transmitted pulse is separated in a second harmonic pulse and a low frequency component. Furthermore the low frequency components in the driven pulse will give rise to Čerenkov-type radiation as this polarization is driven with a velocity $v_x = c/n_{\perp}(\omega)$ with $n_{\perp}^2(\omega) < \epsilon_{||}(0)$. This latter type of behavior was investigated in both theoretical and experimental detail by Auston [13].

One may also expect the nonlinear susceptibility for the difference frequency generation and rectification to differ from that for second harmonic generation, $\chi^{(2)}(0;\omega,-\omega) \neq \chi^{(2)}(-2\omega;\omega,\omega)$. Thus the use of a single real constant $\chi^{(2)}$ in Eq. (1) is no longer justified. The presence of dispersion around the frequencies ω and 2ω, respectively, leads to further corrections, but these will probably not produce significant changes in the pulse behavior. A linear variation of $n_{\perp}(\omega)$ and $n_{||}(2\omega)$ with

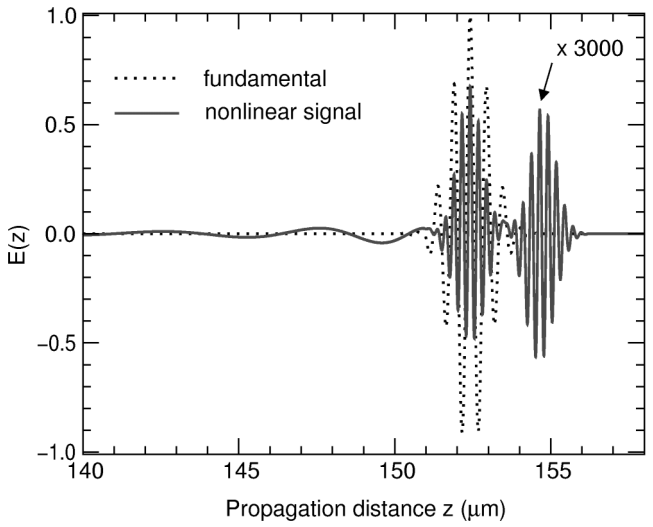

FIG. 4. Temporal splitting of the free and driven second harmonic pulses accompanied by a low frequency tail. The driven second harmonic pulse travels along with the transmitted fundamental pulses which is shown as a dotted line.

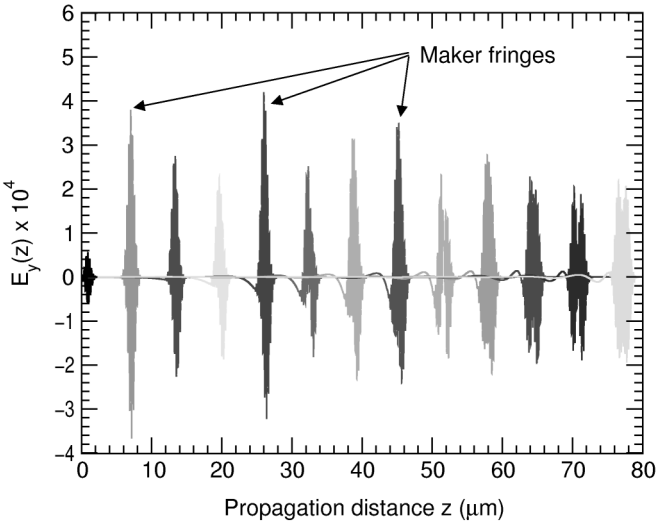

FIG. 5. Series of time snapshots, $E_y(z, t_n)$ versus z for fixed t_n's, of the transmitted second harmonic and low frequency fields as they propagate into the medium. Note the Maker-Terhune oscillations caused by the interference between the free and driven solutions.

ω may be taken into account by group velocity being slightly different from the phase velocity. This will cause a small change in the distance required for separation of the homogeneous and inhomogeneous pulsed solution. Second derivatives of $n_\perp(\omega)$ and $n_{||}(2\omega)$ will cause internal group velocity dispersion leading to distortion of pulse shapes. The distances over which such effects would become significant are generally much longer [3–6] than the coherence length and pulse separation length in our example.

Turning now to the issue of experimental verification of the features described above, let us consider a 20 nJ incident pulse of 10 fs duration, collimated to an area of 1 mm^2. The incident power flux density is 2×10^8 W/cm^2. With $\chi^{(2)} \simeq 8.4 \times 10^{-13}$ m/V one finds from Eqs. (4) and (8) that the forced and free second harmonic transmitted pulse have an energy of about one tenth of a millionth (1.5×10^{-7}) of the incident energy. This would correspond to roughly 6000 second harmonic quanta per pulse which should be readily detectable. We note, however, that the difficulty associated with detecting such weak fields using autocorrelation techniques is probably responsible for the fact that this phenomenon has not previously been observed experimentally.

The time separation between the forced and free pulses could be observed by recombining these transmitted pulses at 2ω with a pulse at ω, split off from the incident pulse, in a thin phase-matched nonlinear platelet to yield an up-converted pulse at 3ω. This signal could be detected by straightforward frequency and spatial filtering as a function of time delay in the path of the reference pulse at ω. Back reflections at the exit surface of the KDP sample could be avoided by antireflective coating on a slightly tilted back surface. The reflected second harmonic pulse energy would be about 3 orders smaller by comparing Eqs. (7) and (8). The signal should still be detectable with a long train of incident femtosecond pulses. One could also use longer incident pulses with 100 fs duration and energy of 200 nJ per pulse.

In conclusion, we have predicted that SHG using femtosecond fundamental pulses produces a pulse splitting of the generated second harmonic field which is of a fundamental nature, that is, it appears even in the absence of material color dispersion and is a product of the basic nonlinear interaction in the phase-mismatched regime. Estimates show that this phenomenon should be observable in current experiments.

Effort sponsored by the Air Force Office of Scientific Research, Air Force Materiel Command, USAF, under Grant No. AFOSR-97-1-0002 and No. AFOSR-98-1-0227.

[1] P. A. Franken, A. E. Hill, C. W. Peters, and G. Weinreich, Phys. Rev. Lett. **7**, 118 (1961).
[2] M. Bass, P. A. Franken, J. F. Ward, and G. Weinreich, Phys. Rev. Lett. **9**, 446 (1962).
[3] E. Sidick, A. Knoesen, and A. Dienes, J. Opt. Soc. Am. B **12**, 1704 (1995).
[4] R. C. Eckhart and J. Reintjes, IEEE J. Quantum Electron. **20**, 1178 (1984).
[5] T. R. Zhang, H. R. Choo, and M. C. Downer, Appl. Opt. **29**, 3927 (1990).
[6] N. C. Kothari and X. Carlotti, J. Opt. Soc. Am. B **5**, 756 (1988).
[7] N. Bloembergen and P. S. Pershan, Phys. Rev. **128**, 606 (1962).
[8] P. D. Maker, R. W. Terhune, M. Nisenoff, and C. M. Savage, Phys. Rev. Lett. **8**, 21 (1962).
[9] N. Bloembergen, H. J. Simon, and C. H. Lee, Phys. Rev. **181**, 1261 (1969).
[10] M. Mlejnek, E. M. Wright, and J. V. Moloney, in *Proceedings of IQEC '98. Summaries of Papers Presented at the International Quantum Electronics Conference*, OSA Technical Digest Series Conference Edition (OSA, Washington, DC, 1998), p. 175; N. Bloembergen, M. Mlejnek, E. M. Wright, and J. V. Moloney, *Advances in Laser Physics*, edited by V. S. Letokhov and P. Meystre (Gordon & Breach, New York, 1999); M. Mlejnek, Ph.D. thesis, University of Arizona, 1998.
[11] D. A. Ledsham, W. G. Chambers, and T. J. Parker, Infrared Phys. **17**, 162 (1977)
[12] K. E. Gauss, H. Happ, and G. Rother, Phys. Status Solidi B **72**, 623 (1975).
[13] D. H. Auston and M. C. Nuss, IEEE J. Quantum Electron. **24**, 184 (1988).